

# Anisotropic polydomain structure in a driven lattice gas with repulsive interaction

György Szabó, Attila Szolnoki, and Tibor Antal

*Research Institute for Materials Science, H-1525 Budapest, P.O. Box 49, Hungary*

(Received 25 May 1993)

Monte Carlo simulations are performed on a square lattice-gas model with a repulsive interaction under the influence of a uniform electric field. Pair-correlation and particle-distribution studies show those polydomain states with strips parallel to the driving field to be stable in the low-temperature region. These results agree with the disappearance of the  $\lambda$  singularity in the specific heat. The formation of the anisotropic polydomain state may be explained by induced interfacial material transport, leading to the instability of planar interfaces.

PACS number(s): 05.60.+w, 05.70.Fh, 68.35.Fx

## I. INTRODUCTION

The driven lattice-gas model was first introduced by Katz *et al.* [1] to describe the particle transport in superionic conductors [2,3]. This model allows us to study the stationary states and the ordering process under the influence of an electric field (for a review see [4]). Monte Carlo (MC) simulations carried out on a half-filled square lattice with attractive nearest-neighbor interaction have shown that the particles segregate into strips parallel to the electric field at low temperatures [1,5]. An exact calculation on a  $2 \times 2$  lattice has confirmed the priority of the parallel interface to the perpendicular one [6]. The stability of the parallel interfaces has been proven by a number of authors [7,8]. The instability of the tilted interface was first shown by Leung [9]. This morphological phenomenon is analogous to the Mullins-Sekerka instability observed in crystallization [10,11] and explains the formation of multistrip states in systems with shifted periodic boundary conditions [12]. Using numerical simulation of the corresponding Cahn-Hilliard equation the initial stage of this anisotropic pattern formation has been studied by Puri *et al.* [13] and Yeung *et al.* [14]

In driven systems the role of inhomogeneities (e.g., density fluctuations, interfaces) becomes very important. Very recently Yeung *et al.* [14,15] have derived an interface description from the Cahn-Hilliard equation and found an instability mechanism due to the enhanced surface current. A much simpler description of this mechanism is suggested by one of us [16]. These theoretical investigations explain the formation of multistrip states in such systems where the particle current is localized at the interfaces because the instability and the ensuing processes cut the large domains into strips parallel to the driving field.

Half-filled driven lattice-gas models with repulsive interaction have also been studied by several authors. In such systems the theoretical approximations suggest an ordering process corresponding to the formation of a monodomain chessboardlike particle distribution. According to the dynamical mean-field theories [17,18] and the renormalization-group calculation [19], the transition temperature decreases with the electric field: it becomes

zero above a threshold value and the ordering is completely suppressed in the strong-field limit. Analysis of the critical behavior has shown that this driven system belongs to the (equilibrium) Ising universality class [19]. Although several MC simulations [1] were performed on this system with repulsive interaction the theoretical predictions have not yet been checked quantitatively. The present work was initiated because of this deficiency.

Our MC simulations, however, do not confirm the basis of the theoretical descriptions mentioned above. Instead of an ordered monodomain state we observed the formation of an anisotropic polydomain state which is found to be stable at low temperatures. This phenomenon is induced by the interfacial material transport as has already been described in the driven systems with attractive interaction [14–16]. The enhanced material transport along the “grain boundary” results in the instability of planar interfaces and prevents the formation of large domains. Consequently, the correlation lengths do not diverge; there is no critical behavior. The system transforms continuously into a self-organizing, anisotropic polydomain state at low temperatures. During this process the equilibrium  $\lambda$  singularity of specific heat becomes a wide peak.

In the present work the stationary polydomain state is studied by determining the transverse and longitudinal correlation lengths. Our simulations are carried out on a system whose sizes are chosen to be much larger (as large as  $300 \times 1000$ ) than the corresponding correlation lengths (or domain sizes). This condition is not satisfied in previous MC simulations [1,5] which suggest (in contrast to our results) stable monodomain state and isotropy in the low-temperature region. It is emphasized that the monodomain state is not affected directly by the mentioned interfacial instability therefore it may be observed for a long time. However, there exists a nucleation mechanism which is supported by the induced interfacial current and this can lead to a transition of the monodomain to the stationary, polydomain state, as discussed later. The efficiency of this mechanism depends strongly on the temperature and field strength. The formation of the anisotropic, polydomain structure from a monodomain state becomes very slow at low tempera-

tures and its rigorous investigation is beyond our computer capacity.

In the next section we present the results of MC simulations. An analytical description of the interfacial instability is given in Sec. III. The alternative picture of the stationary states in the present driven lattice-gas model is summarized in Sec. IV.

## II. MONTE CARLO SIMULATIONS

We consider a lattice-gas model with repulsive nearest-neighbor interaction on a square lattice for a fixed concentration  $c = 1/2$ . The Hamiltonian is given by

$$H = J \sum_{\langle i,j \rangle} n_i n_j, \quad (1)$$

where  $n_i = 1$  for an occupied site,  $n_i = 0$  for an empty site and the sum is over the nearest-neighbor pairs. In the lattice the particles can jump to one of the empty nearest-neighbor sites. The jump rate from site  $i$  to  $j$  is biased by a vertical electric field  $E$ , namely,

$$\Gamma(i \rightarrow j) = \frac{1}{1 + \exp[(\Delta H - E\Delta y)/T]}, \quad (2)$$

where  $\Delta H$  is the energy difference between the final and initial states,  $\Delta y$  is the vertical component of displacement, and  $T$  is the temperature. For simplicity we choose many parameters (i.e., coupling and lattice constants, electric charge, Boltzmann constant) to be unity. (For details of MC simulations see the review by Binder and Stauffer [20].)

In the simulations we have used a rectangular box of  $L \times M$  sites with periodic boundary conditions. The sizes are chosen to be greater than ten times the corresponding correlation lengths. More precisely,  $L = M = 300$  for high temperatures ( $T > T_c = 0.576$ ) and the longitudinal length is increased at low temperatures, e.g.,  $M = 1000$  for  $T < 0.42$ . To reach the stationary state the system is thermalized for typically 10 000–50 000 MC steps per particle (MCS). Most of our simulations are carried out for a fixed driving field  $E = 0.4$ .

Figure 1 displays a typical particle distribution for  $E = 0.4$  and  $T = 0.42$ . To visualize the domain structure of sublattice orderings the particles are illustrated by boxes whose size depends on the sublattice they are staying at the given time. This trick results in a different gray scale in the phases *A* and *B* as demonstrated in Fig. 1. We could not observe any changes in the typical domain sizes from  $t = 5000$  MCS to  $t = 1.2 \times 10^6$  MCS. Here it is worth mentioning that similar domain structure has been found under the same conditions when using the Metropolis jump rate instead of the Kawasaki transition rate given by Eq. (2). Decreasing the temperature the anisotropy of domain structure becomes more and more striking.

During the simulations we evaluated the pair correlations,

$$g(r) = \frac{\langle n_0 n_r \rangle - \langle n_0 \rangle \langle n_r \rangle}{\langle n_0 \rangle \langle n_r \rangle} \quad (3)$$



FIG. 1. Particle distribution and domain structure in the presence of a vertical field  $E = 0.4$  for  $T = 0.42$ . A  $200 \times 300$  portion of the full  $256 \times 512$  lattice is shown. The different gray scale of domains is a consequence of the particle sizes dependent on the sublattice.

along the longitudinal and transverse directions where the indices 0 and  $r$  refer to sites on the same sublattice. For high temperatures the pair correlation decreases exponentially, i.e.,  $g(r) \propto \exp(r/\xi)$ . The longitudinal and transverse correlation lengths ( $\xi$ ) are determined by a fitting to MC data obtained by averaging over 200 000 MCS. For low temperatures, however, an oscillation may be observed in the transverse pair correlation, see curve *b* in Fig. 2. Similar behavior has been found by Vallés and Marro [5] when studying the multistrip state in the driven lattice gas with attractive interaction.

A series of MC simulations was carried out to determine the temperature dependence of the correlation lengths. For low temperatures the transverse correlation length is estimated from those data which satisfy the condition  $g(r) > 0.05$ . The results are illustrated in Fig. 3. This figure demonstrates that the driven system remains isotropic above the equilibrium  $T_c$ . On decreasing the temperature the transverse correlation (strip width) tends to be constant whereas the longitudinal correlation increases monotonically. From the present data we cannot conclude the singularity of the longitudinal correlation length for finite temperature. Unfortunately, the

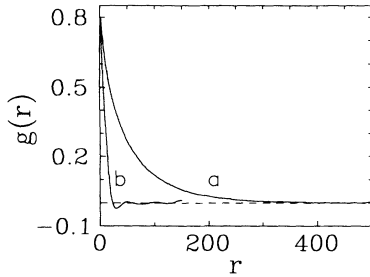


FIG. 2. Pair correlation along the longitudinal (curve *a*) and transverse (curve *b*) directions for  $T = 0.39$  and  $E = 0.4$ . The MC simulation is performed on a lattice of  $300 \times 1000$  sites, the average is taken over 500 000 MCS.

simulations for lower temperatures require a long time because we need to increase the longitudinal box size ( $M$ ) in order to avoid the disadvantageous effect of periodic boundary conditions. The size effect has been checked for several temperatures. It is found that the results obtained for larger systems agree with the plotted ones within the statistical error whose value is indicated by the symbol sizes in the figures.

Several simulations are performed for  $E = 0.2$  and  $0.6$ . Although the preliminary results suggest similar behavior, the typical strip width increases when decreasing the driving field.

During the above simulations the system energy was also monitored. By this means we could evaluate the average energy as a function of temperature. From this data the specific heat is determined by a simple numerical derivation. It is worth mentioning that here the specific heat may not be derived from the energy fluctuations because the fluctuation-dissipation theorem does not apply in driven systems [5]. The results are indicated by the filled circles in Fig. 4. For comparison the equilibrium specific heat was also determined by using the same method for  $E = 0$  and  $L = M = 200$  (see boxes in Fig. 4). The contrast is conspicuous, the critical behavior is suppressed by the driving field. This result is in close agreement with the absence of singularity in the correlation lengths (see Fig. 3). As expected, the temperature dependence of specific heat becomes sharper and the peak position tends towards the equilibrium  $T_c$  for  $E = 0.2$ .

The disappearance of critical behavior may be ex-

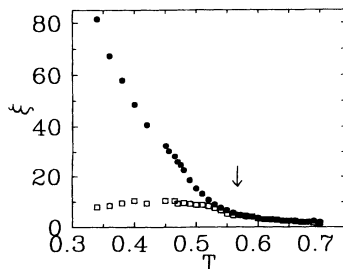


FIG. 3. Longitudinal ( $\bullet$ ) and transverse ( $\square$ ) correlation lengths vs temperature for fixed external field  $E = 0.4$ . The equilibrium critical temperature is indicated by an arrow.

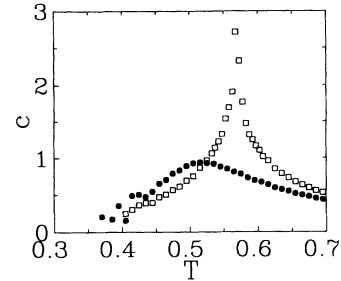


FIG. 4. Specific heat of equilibrium ( $\square$ ) and driven ( $\bullet$ ) lattice gas for  $E = 0.4$ .

plained by the instability of the planar interfaces, as is discussed in the next section.

### III. INTERFACIAL INSTABILITY

If one displays the time evolution of particle distribution, one can easily observe that the particle transport is localized at the interface separating the ordered phases *A* and *B*. The interfacial current is determined by the component of external field parallel to the interface. Consequently, the current varies along a curved interface and the inhomogeneous current leads to the formation of regions with extra particles or holes (see Fig. 5). The interface regions with extra particles (holes) are driven upwards (downwards) leaving an ordered structure behind. This mechanism drives the instability of the planar interfaces.

The destabilizing effect of the interfacial current may be described by introducing a simple formalism based on the neglecting of interface thickness between the ordered phases. In this case the interface evolution is given by a curve  $\zeta(x, t)$  in the two-dimensional Cartesian coordinate system. The variation of the extra charge density  $\varrho(x, t)$  on the interface is determined by the interfacial current  $j(x, t)$  induced by the vertical field  $E$ , namely,

$$\partial_t \varrho = -\partial_x j(x, t), \quad (4)$$

where  $\partial_t$  and  $\partial_x$  denote the partial derivatives with respect to time and the  $x$  coordinate. We assume that the current  $j(x, t)$  is proportional to the gradient of chemical

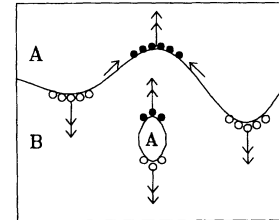


FIG. 5. Schematic plot of interfacial instability. The solid lines indicate the interfaces between the ordered phases *A* and *B*, bullets and open circles represent extra particles and holes. The arrows show the direction of interfacial current, the double arrows the motion of interface.

potential  $\mu(x, t)$  for the interfacial particles, that is,

$$j(x, t) = -\sigma \frac{d\mu}{ds} = \frac{-\sigma \partial_x \mu}{[1 + (\partial_x \zeta)^2]^{1/2}}, \quad (5)$$

where  $s$  refers to the derivation with respect to arclength along the interface and  $\sigma$  characterizes the (isotropic) interfacial conductivity. The chemical potential is given by a simple expression

$$\mu(x, t) = -E\zeta + \frac{D\rho}{[1 + (\partial_x \zeta)^2]^{1/2}}, \quad (6)$$

where the first term is the contribution of the vertical field  $E$ . The second term is introduced to describe the diffusion along the interface ( $D > 0$ ). In the absence of an electric field this term results in a homogeneous interfacial charge density ( $\rho = 0$  for  $c = 1/2$ ). In the above description we have neglected the variation of charge density caused by the interfacial evolution.

In the present lattice-gas model the bulk conductivity strongly depends on the concentration at low temperatures. It has a sharp minimum at the concentration  $c = 1/2$  we are interested in. Consequently, the regions with extra particles ( $c > 1/2$ ) are driven along the field. Due to the particle-hole symmetry the extra holes are driven opposite to the field. In agreement with this feature here we assume that the normal velocity of the interface  $v_n = \nu E_n \rho_0$ , where  $E_n$  is the normal component of the electric field,  $\rho_0$  is the charge density along the interface, and  $\nu > 0$  may be considered as the mobility of the interface. For  $E = 0$  the motion of interfaces is determined by the surface tension as it was first described by Allen and Cahn [21]. These theoretical investigations suggested that the normal velocity of the interface is proportional to the curvature, i.e.,  $v_n = C \partial_{xx}^2 \zeta / [1 + (\partial_x \zeta)^2]^{3/2}$  where coefficient  $C$  is related to the surface tension [21,22]. These mechanisms are combined in the following simple equation of motion:

$$\partial_t \zeta = \frac{\nu E \rho}{[1 + (\partial_x \zeta)^2]^{1/2}} + C \frac{\partial_{xx}^2 \zeta}{[1 + (\partial_x \zeta)^2]}. \quad (7)$$

In the above expressions the parameters may depend on the temperature and electric field. In the low-field limit, however, the field dependence is negligible. Substituting Eqs. (6) and (5) into Eq. (4) the differential equations (4) and (7) have a trivial solution,

$$\zeta_0(x, t) = y_0 + mx, \quad (8)$$

$$\rho_0(x, t) = 0, \quad (9)$$

corresponding to a neutral, tilted, planar interface with slope  $m$ . The linear stability analysis of this interface may be carried out by assuming a small periodic perturbation, i.e.,

$$\zeta(x, t) = \zeta_0 + \delta_1 e^{\lambda t + ikx}, \quad (10)$$

$$\rho(x, t) = \rho_0 + \delta_2 e^{\lambda t + ikx}, \quad (11)$$

where  $|\delta_1|, |\delta_2| \ll 1$  and  $k$  is the wave number. The amplification rate  $\lambda$  may be determined by linearizing Eqs. (4) and (7). From these linearized equations one

can obtain two solutions:

$$\lambda_{1,2} = -\frac{(C + \sigma D)k^2 \pm \sqrt{(C - \sigma D)^2 k^4 + 4\sigma \nu E^2 k^2}}{2(1 + m^2)}. \quad (12)$$

It is easy to see that  $\lambda_1 > 0$  for  $|k| < k_0$  if  $E \neq 0$  where  $k_0^2 = E^2 \nu / DC$  and  $\lambda_2 \leq 0$  for arbitrary  $k$ . This result demonstrates that the planar interface is unstable against infinitesimal fluctuations for sufficiently long wavelengths. In the limit  $k \rightarrow 0$ ,  $\lambda_1 \propto |Ek|$  and  $\lambda_1 \propto -k^2$  in the short wavelength region. This calculation suggests no phase difference in the oscillation of  $\zeta$  and  $\rho$  for the increasing modes. In the suppressed modes corresponding to  $\lambda_2$ , however,  $\zeta$  and  $\rho$  oscillate with opposite phases. It is emphasized that the oscillations of  $\zeta$  and  $\rho$  are decoupled for  $E = 0$ .

Equation (12) illustrates that the maximum value of  $\lambda$  is reached for  $m = 0$ . The amplification rate is decreased for the interfaces which are not perpendicular to the driving field. More precisely, the instability vanishes for  $m = \infty$ , that is, the interfaces parallel to the driving field remain stable.

Similar interfacial instability has been found for the driven systems corresponding to the lattice gases with attractive interaction [14–16]. However, a significant difference may be observed in the  $k$  dependence of  $\lambda$  when comparing the two systems. An analogous description suggests  $\lambda \propto Ek^2(k_0^2 - k^2)$  for the systems with attractive interaction [16]. Consequently, the attractive system exhibits a sharper maximum in  $\lambda(k)$ . At the same time, the maximum value of  $\lambda$  is proportional to  $E^2$  in both driven systems.

The instability of the planar interface has serious consequences. This process may be considered as the initial stage of an interface evolution cutting the large domains into strips while the interfaces parallel to the driving field remain stable. According to this picture, the typical strip width is strongly related to the inverse of the wave number which is characterized by the largest positive  $\lambda$ . Consequently, the typical strip width is expected to be proportional to  $1/|E|$ . The finite strip size along the field may be explained by the interface fluctuations whose effect is neglected in the above description.

The (low-temperature) monodomain structure does not have a widespread interface that may be attacked by the instability induced by the driving field. In this state, however, the interfacial current can polarize the small island of the other phase (see Fig. 5) formed randomly in the system. The growth of polarized islands is driven by the same mechanism described above. This phenomenon may easily be observed in MC simulations when choosing, for example,  $T = 0.42$  and  $E = 0.4$ .

The instability of the planar interface and the growth of the “polarized islands” result in a stationary state with striplike domains. More precisely, the competition between the traditional domain growth and the above interfacial instability leads to a “self-organizing” anisotropic polydomain state. A better understanding of the interface evolution, however, requires further analysis taking into account nonlinearity, anisotropy, fluctuations, interface thickness, etc.

#### IV. CONCLUSIONS

Using MC simulations we have studied the stationary states in a half-filled driven lattice-gas model with repulsive nearest-neighbor interaction. In comparison with the equilibrium state the driving field caused significant changes in the stationary state at low temperatures. Instead of the ordered monodomain state we observed a “self-organizing” polydomain structure if the system sizes are chosen to be much larger than the typical domain sizes. This domain structure is strongly anisotropic; the ratio of the longitudinal and transverse sizes depends on the temperature and field strength. The present simulations suggest that the transverse domain size (correlation length) tends to be constant if one decreases the temperature for fixed driving fields. At the same time, the longitudinal size of a typical domain increases.

In these anisotropic polydomain structures the traditional ordering is prevented by the driving field when decreasing the temperature. Suppression of the critical behavior is clearly demonstrated by the disappearance of singularity in the specific heat.

The anisotropic polydomain structure has been found to be stable for low temperatures. In this temperature region the previous theoretical investigations suggested a homogeneous state with long-range order. This expectation is motivated by the fact that during traditional ordering ( $E = 0$ ) the polydomain structures transform into a monodomain one via a domain growth mechanism. In driven systems, however, the domain growth is strongly affected by the interfacial material transport. The induced particle current produces a charge redistribution along the interface whose motion is determined by the accumulated particles or holes. Neglecting bulk diffusion and interface thickness we suggest a very simple model to describe the initial stage of this process. This description is restricted to the low-field (Ohmic) region. The present model explains the instability of those planar interfaces which are not parallel to the driving field. The instability and the ensuing processes prevent the formation of large domains. This phenomenon may easily be observed in MC simulations for  $T < 0.8T_c$  and  $E \approx 0.5$  if the system is started from a two-domain state with planar interfaces perpendicular to the driving field [23].

We have concluded that competition between the traditional domain growth mechanism and the interfacial instability controls the stationary domain structure. This conclusion is confirmed by MC simulations performed on suitably large systems. For small systems the longitudi-

nal strip size may exceed the (fixed) box size and the periodic boundary conditions result in closed strips on the torus. In this domain structure the interfaces are parallel to the driving field therefore they are not attacked by the instability mentioned above. In this case the random motion of the interfaces increases or decreases the strip widths. As a result a strip domain may disappear and the average strip width increases with time. Finally the system can transform into a monodomain state if the process is not prevented by the nucleation mechanism mentioned above. This phenomenon has also been observed in our simulations when visualizing the evolution of planar interfaces for low temperatures and small sizes. This process resolves the discrepancy found in relation to our results for previous simulations.

The effect of interfacial transport on the domain structure is not restricted to the present two-dimensional model. Similar phenomena are expected to appear for higher dimensions.

The enhanced interfacial transport is responsible for the instability of the planar interfaces in driven lattice gases with either attractive or repulsive interaction. The analytical investigation of this phenomenon has cleared up the differences between the two systems. On the one hand, the equation of motion of the interfaces is derived from a conservation law for the systems with attractive interaction. Here, the interfacial current destabilizes the interfaces if the field drives the particles out of the surface. For a reversed field the interface is stabilized by this mechanism. A linear stability analysis suggests that the typical strip width is proportional to  $1/\sqrt{E}$ . On the other hand, the interfacial evolution is coupled to the variation of charge density along the interface if the interaction is repulsive. The ordered phases ( $A$  and  $B$ ) separated by the interface are equivalent, therefore the mechanism remains unchanged when reversing the field direction. This more complicated mechanism leads to a different  $k$  dependence of amplification rate suggesting the characteristic strip width to be proportional to  $1/|E|$ . It is emphasized that both mechanisms predict increasing strip width if  $E \rightarrow 0$ , that is, the transition from anisotropic polydomain to monodomain state is continuous when decreasing the driving field.

#### ACKNOWLEDGMENTS

This research was supported by the Hungarian National Research Fund (OTKA) under Grant No. T-4012.

- 
- [1] S. Katz, J. L. Lebowitz, and H. Spohn, *Phys. Rev. B* **28**, 1655 (1983); *J. Stat. Phys.* **34**, 497 (1984).
  - [2] See, e.g., S. Chandra, *Superionic Solids* (North-Holland, Amsterdam, 1981).
  - [3] W. Dieterich, P. Fulde, and I. Peschel, *Adv. Phys.* **29**, 527 (1980).
  - [4] B. Schmittman, *Int. J. Mod. Phys. B* **4**, 2269 (1990).
  - [5] J. L. Vallés and J. Marro, *J. Stat. Phys.* **49**, 89 (1987).
  - [6] G. Szabó, A. Szolnoki, and G. Ódor, *Phys. Rev. B* **46**, 11 432 (1992).
  - [7] K.-T. Leung, *J. Stat. Phys.* **50**, 405 (1988).
  - [8] A. Hernández-Machado and D. Jasnow, *Phys. Rev. A* **37**, 656 (1988).
  - [9] K.-T. Leung, *J. Stat. Phys.* **61**, 345 (1990).
  - [10] W. W. Mullins and R. F. Sekerka, *J. Appl. Phys.* **34**, 323 (1963); **35**, 444 (1964).
  - [11] J. S. Langer, *Rev. Mod. Phys.* **52**, 1 (1980).
  - [12] J. L. Vallés, K.-T. Leung, and R. K. P. Zia, *J. Stat. Phys.*

- 56**, 43 (1989).
- [13] S. Puri, K. Binder, and S. Dattagupta, *Phys. Rev. B* **46**, 98 (1992).
- [14] C. Yeung, T. Rogers, A. Hernández-Machado, and D. Jasnow, *J. Stat. Phys.* **66**, 1071 (1992).
- [15] C. Yeung, J. L. Mozos, A. Hernández-Machado, and D. Jasnow, *J. Stat. Phys.* **70**, 1149 (1993).
- [16] G. Szabó, *Phys. Rev. E* (to be published).
- [17] R. Dickman, *Phys. Rev. A* **41**, 2192 (1990).
- [18] A. Szolnoki and G. Szabó, *Phys. Rev. E* **48**, 611 (1993).
- [19] K.-T. Leung, B. Schmittmann, and R. K. P. Zia, *Phys. Rev. Lett.* **62**, 1772 (1989).
- [20] K. Binder and D. Stauffer, in *Applications of Monte Carlo Methods in Statistical Physics*, edited by K. Binder, Topics in Current Physics Vol. 36 (Springer-Verlag, Berlin, 1983), p. 1.
- [21] S. M. Allen and J. W. Cahn, *Acta Metall.* **27**, 1085 (1979).
- [22] K. Kawasaki and T. Ohta, *Prog. Theor. Phys.* **67**, 147 (1982).
- [23] G. Szabó, A. Szolnoki, A. Tibor, and I. Borsos, *Fractals* (to be published).